EMERGING MINDS
JOURNAL FOR STUDENT RESEARCH

ISSN 2976-9094
EMJSR 2024,Vol 2 (1):78-102
https://doi.org/10.59973/emjsr.110

Received: 2024-06-07
Accepted: 2024-07-10
Published: 2024-07-11

The Equivalence Circuit Model for Lithium-ion Batteries

Aysha Fathealdeen[1,*]

[1]University of Portsmouth, School of Mathematics and Physics, Portsmouth, PO1 3FX, United Kingdom

*Corresponding author: aysha$_a$*ldeen@hotmail.com*

Abstract -This study analyzes equivalent circuit models for lithium-ion batteries to simulate voltage behavior under various C-rates. Starting with a simple SOC to voltage model and progressing to Thevenin and PNGV models, it finds that more complex models perform better. Implemented in Python using Dandeliion , the study compares simulated outputs with experimental data, discussing accuracy, complexity, and computational cost. It aims to identify the simplest model that effectively captures voltage dynamics, provide suggestion based on C-rate and desired accuracy, and emphasise the validation of simplified models against experimental data.

Keywords - Equialent Circuit Model, LiB Batteries, Circuit Models.

1 Introduction

LiB batteries are the most widely used in electric vehicles, electric equipment, and handheld electronic devices. For example, hybrid/electric vehicles, E-scooters, power tools, laptops, and smartphones. With these, we must ensure that the safety of these batteries does not fail and endanger the general public since there have been recent talks about E-scooter explosions. The causes can range from production flaws to battery abuse. Nevertheless, this just demonstrates a huge demand for LiB and research into ways to make it more efficient in terms of storage capacity and the speed at which it can be charged and refilled, ensuring the safety of these batteries so that a fault doesn't occur. Lithium-ion batteries are made up of two electrodes, a separator, electrolyte, and two current collectors. he two electrodes are the cathode, which is the positive electrode, and the anode which is the negative electrode. the electrolyte permits the anode, and cathode to exchange electrical charge in the form of lithium ions.

Different types of LiB each have their distinct advantages and trade-offs, suited for varied applications. Cylindrical cells, known for their metal-clad tubular design, offer manufacturing ease and cost efficiency. Yet, their shape may result in suboptimal space utilization, posing challenges for space-constrained applications. Prismatic lithium-ion cells, with their space-saving rectangular design, are ideal for compact devices, although they tend to have lower energy density and heat management challenges compared to cylindrical cells. Button cells, characterized by their coin-like shape and compactness, suit low-power devices such as watches and hearing aids, but their limited capacity and higher resistance restrict their use in high-power applications. Pouch lithium-ion cells offer design flexibility and are cost-effective, making them popular for consumer electronics and electric vehicles.

2 The Equivalence Circuit Model

2.1 Why choose ECM?

The behaviour of batteries, particularly LiB, is described and predicted using two mathematical approaches: physics-based electrochemical models and equivalent circuit models such as [17, 10] (ECMs). When comparing the two, both have pros and cons, however, here's why ECMs are generally preferred for particular applications:

Physics-based electrochemical models such as Doyel Fuller Newman type models [7, 8, 9] use complex equations (coupled partial differential equations) to provide extensive insights into battery chemistry and internal operations, which makes them very accurate but computationally intensive, meaning a longer runtime. These models are useful for research and development requiring a thorough understanding of battery behaviour. In this model, fully parameterized cells are required, necessitating 30 parameters. This process is costly, and companies typically keep such information confidential, limiting public access.

On the contrary, Equivalent circuit models (ECM)[4] employ less complex representations, such as resistors, capacitors, and voltage sources, to simulate battery behaviour. ECMs are easier to use, require less computational power, and are quick enough for real-time applications like battery management systems in electric vehicles. While they offer less detail compared to physics-based models, ECMs provide sufficient accuracy for operational management and are adaptable to different battery types and conditions.

ECM's are commonly used in practical applications because they offer a good combination of simplicity, computing efficiency, and sufficient predictive skills. This makes them well-suited for real-time monitoring and control situations where resources and rapid estimations are important. For these reasons, this model is highly favoured in today's industry.

In this study, I will employ circuit models rather than physics-based models for several compelling reasons, which were previously discussed. Additionally, I will demonstrate the effectiveness of the circuit model approach. In the following section, we will revisit Kirchhoff's laws as outlined in the literature.

3 Kirchhoff's law

3.1 Kirchhoff's voltage law [3, 2]

Kirchhoff's voltage law (KVL) asserts that the sum of all electrical voltages surrounding any closed loop in a circuit is zero. This equation is based on the principle of energy conservation, which states that the total energy received by charges in a loop must equal the total energy lost as they return to their original location. In other words, in a closed circuit loop, the sum of potential rises (voltage gains) must equal the sum of potential drops (voltage losses). In mathematics, it can be stated as:

$$\sum_{k=1}^{n} V_k = 0 \tag{1}$$

Where V_k represents the voltage (gain or a loss) at k^{th} element within the loop. n represents the total number of elements in the loop.

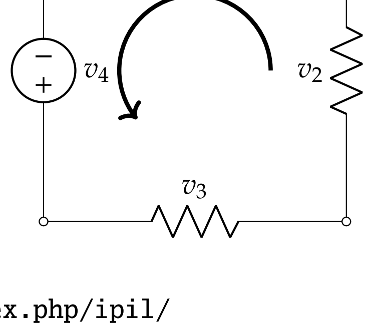

This figure illustrates a circuit that follows Kirchhoff's voltage law, which states that the sum of the voltages in a closed loop is equal to zero. In this circuit, the voltages v_1, v_2, v_3, and v_4 are combined in such a way that their sum is zero.

3.2 Kirchhoff's current law

According to Kirchhoff's Current Law (KCL), the total current entering a junction or node in an electrical circuit must be equal to the total current exiting the node. This law is based on the charge conservation principle, which states that charge cannot accumulate at a junction; in other words, what goes in has to come out. KCL can be stated mathematically as follows:

$$\sum_{k=1}^{n} I_k = 0 \tag{2}$$

Where I_k reflects the current flowing into or out of the node (currents entering the node are regarded positive, while currents exiting the node are considered negative). n represents the total number of branches connecting to the node.

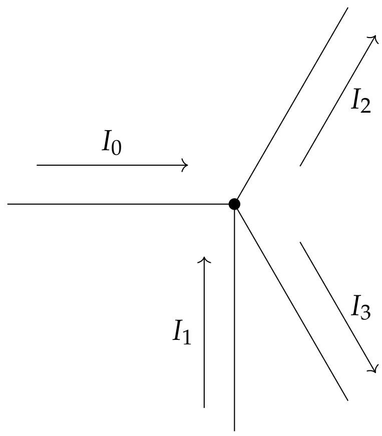

Kirchhoff's current law, seen in this picture, asserts that the sum of currents entering any junction is equal to the sum of currents exiting that junction, expressed as $I_0 + I_1 = I_2 + I_3$. Rearranging this equation yields a sum equal to zero.

The Equivalence Circuit Model for lithium-ion batteries: We will begin with the fundamental electrical circuit model, which reflects a basic grasp of the constituents and functionality of an electrical circuit in a straightforward and comprehensible manner [18]. With an electrical circuit; electric current can flow through and through each component.

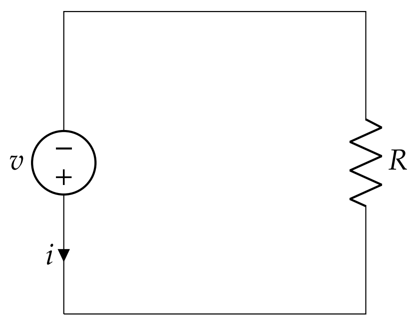

An active system has at least one voltage or current source capable of supplying energy eternally. A passive system does not contain an active source . This circuit's behaviour may be analysed using Kirchhoff laws, which relates voltage (V), current (I), and resistance (R) in a linear relationship ($V = IR$). This fundamental law is essential for understanding how changes in one component of the circuit can affect the entire system.

In the next section, we will begin constructing the Equivalent Circuit Model (ECM) for the LiB. To facilitate this, we will introduce several key definitions.

4 Building The ECM

Open-circuit voltage (OCV): OCV is an indicator of a battery's charge condition. The OCV of rechargeable batteries, including lithium-ion batteries, fluctuates based on the battery's level of charge. As it rises when charging and decreases during discharging, this figure can be used to estimate the battery's remaining energy.

State of Charge (SOC): The state of charge (SOC) indicates how much charge remains in the battery, reflecting its ability to produce power when connected to a load. This measurement is critical for assessing the battery's health and efficiency, as well as determining energy consumption and charging schedules.

Equation for SOC: The State of Charge (SOC) for a cell, denoted as $z(t)$, is described. When cell is fully charged then $z(t) = 100\%$, in contrast to a completely discharged cell, where $z(t) = 0\%$. Based on this information, we can model SOC by following equation:

$$\frac{dz}{dt} = \frac{-I(t)}{Q} \tag{3}$$

$$\int_{t_0}^{t} dz = \int_{t_0}^{t} \frac{-I(t)}{Q} dt \tag{4}$$

$$z(t) = z(t_0) - \frac{1}{Q} \int_{t_0}^{t} I(t)dt \tag{5}$$

$I(t)$ the current at time t (positive for discharge, negative for charge). Nevertheless, it should be noted that cells are not flawless and invariably possess a coulombic efficiency, represented by the efficiency factor $\eta(t)$:

$$\frac{dz}{dt} = \frac{-I(t)\eta(t)}{Q} \tag{6}$$

$$z(t) = z(t_0) - \frac{1}{Q} \int_{t_0}^{t} I(t)\eta(t)dt \tag{7}$$

By applying initial conditions, we can solve Equation (7). Given the large dataset in reality, we will employ numerical methods to solve for $z(t)$.

The efficiency with which charge is moved in and out of a battery during the charging and discharging cycles is known as "coulombic efficiency," or $\eta(t)$. When charging, $\eta(t)$ is typically less than 1 (usually about 99%) due to losses from unwanted side reactions; however, it is generally modeled as 1 during discharge, indicating no loss of charge.
It is important not to confuse coulombic efficiency with energy efficiency. While coulombic efficiency represents the ratio of charge output to charge input, energy efficiency, which accounts for about 95%, measures the ratio of energy output to energy input. The discrepancy in energy efficiency primarily stems from resistive heating, which results in energy loss, though the charge itself is not lost [4].

Additionally, we will validate the analytical solution by comparing it with our numerical results. Specifically, we will use the first-order Euler forward method for this purpose.

Euler forward method: This method is a straightforward numerical procedure used to approximate the solutions of ordinary differential equations (ODEs). [22]. In the next paragraph, we will recall Euler's forward method for ODE.

Using the first-order differential equation:

$$\frac{dy}{dt} = f(t, y(t)) \tag{8}$$

y is the variable of interest. When applying Euler forward method we first start from an initial condition $y(t = t_0) = y|_{t=t_0} = y_0$ and use the equation:

$$\frac{y(t_0 + \Delta t) - y(t_0)}{\Delta t} = f(t_0, y(t_0)) \tag{9}$$

$$y(t_0 + \Delta t) = y(t_0) + \Delta t f(t_0, y(t_0)) \tag{10}$$

Similarly we can write for the t^{th} iteration

$$y(t_{i+1}) = y(t_i) + \Delta t f(t_i, y(t_i)) \tag{11}$$

$$y(t + \Delta t) = y(t) + \frac{dy}{dt} \cdot \Delta t \tag{12}$$

Δt is a time step where it's in a small increment over which you approximate the change in y. The choice of Δt affects the accuracy and stability of the method.

By establishing initial circumstances to facilitate the integration process, the equation $t = t_0$ ensures that the state of charge is equal to z_0 at time t_0.

The Forward Euler method calculates the updated solution of the ordinary differential equation (ODE) using the following formula:

$$z(t + \Delta t) = z(t) - \frac{I(t)\eta(t)}{Q} \cdot \Delta t \tag{13}$$

$z(t + \Delta t)$ is the approximation of the state of charge at the next time step. The table below presents a simplified overview of the parameters:

Variables/Parameters	Unit/Dimension	Values
Q : Capacity	Amp hour/Ah	$0 - 100$
I : Current	Amp/A	$0 - 10$
$z(t)$: SOC	Dimensionless	unknown
$z(0) = z(t = 0)$: Initial SOC	Dimensionless	0
t : Time	Hour/ second	$1 - 10$
η: Coulombic efficiency	Dimensionless	$0 - 1$

From this we can give an example of the parameters being $Q = 90Ah, I = 10A, z(0) = 0.8, \eta = 0.95, t = 10$ plugging in the values in the Forward Euler method :

$$z(t + \Delta t) = z(t) - \frac{10 \times 0.95}{90} \cdot \Delta t = z(t) - 0.1056 \cdot \Delta t \tag{14}$$

$$z(0.1) = 0.8 - 0.1056 \cdot 0.1 = 0.78944 \tag{15}$$

$$z(0.2) = 0.78944 - 0.1056 \cdot 0.1 = 0.77888 \tag{16}$$

$$z(0.3) = 0.77888 - 0.1056 \cdot 0.1 = 0.76832 \tag{17}$$

We can see the state of charge is decreasing over time, and when it's at 10 hours we get:

$$z(10) = 0.8 - 0.1056 \cdot 10 = -0.256 \tag{18}$$

Based on this, it is possible to develop a Python script with different I values:

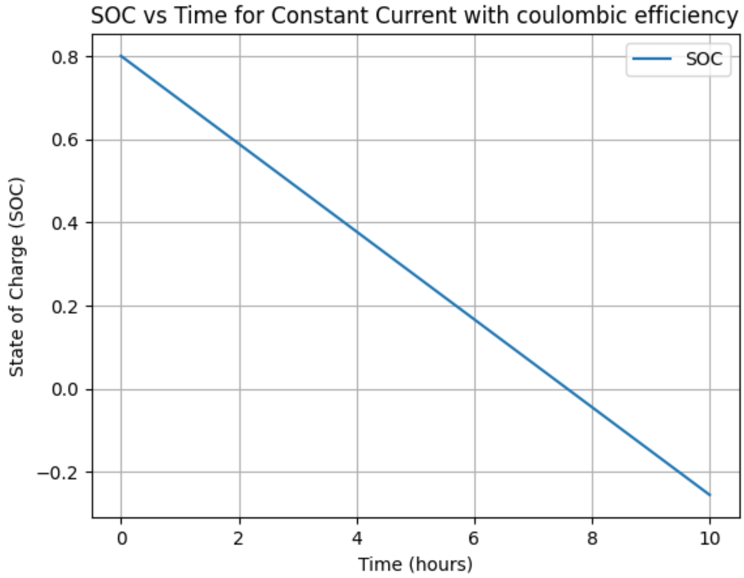

Figure 1: State of Charge (SOC) decreases over time when I is at 10A"

With the parameters being $Q = 90, I = 10, z(0) = 0.8, \eta = 0.95, t = 10$. When the current is flowing at constant at 10 [Amps], the battery's charge is continuously drained, demonstrating a consistent discharge rate with no efficiency loss or increase over time. As the SOC falls below zero, which should not happen in a real-world scenario; this is an example of what would happen if the battery was 'used' beyond its drained state. which we have predicted as shown above. Now we will give a simple example to show the comparison between our numerical method and analytical solution of ODE.

Example: Comparison between analytical and numerical solution. For the Analytical solution we will use (4), the parameters we will use are :

$$z_0 = 0.8,\ Q = 1,\ \eta = 1, I = 2,\ t = 1$$

plugging in the values in the Forward Euler method :

$$z(t + \Delta t) = z(t) - \frac{2 \times 1}{1} \cdot \Delta t = z(t) - 2 \cdot \Delta t \tag{19}$$
$$z(0.1) = 0.8 - 2 \cdot 0.1 = 0.6 \tag{20}$$
$$z(0.2) = 0.6 - 2 \cdot 0.1 = 0.4 \tag{21}$$

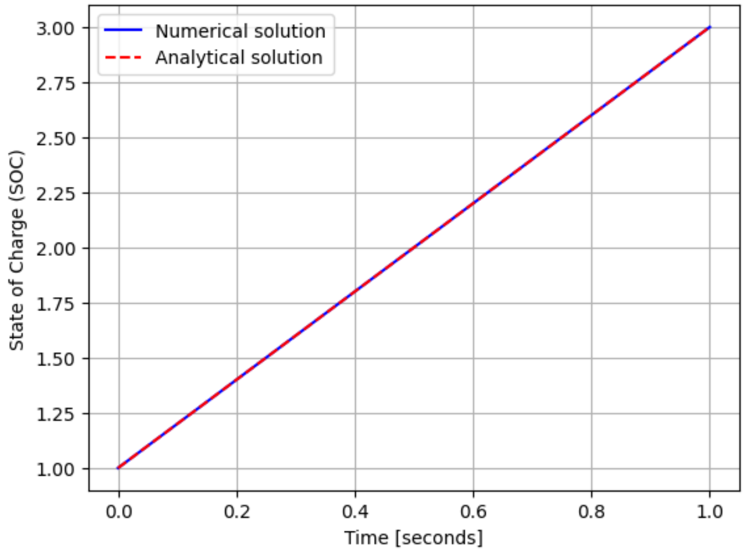

Figure 2: Battery State of Charge Increment Over Time: Numerical vs. Analytical solution

In figure 2 the "numerical solution" (blue) and the "analytical solution" (red dashed line). Both lines show a linear relationship between SOC and time, implying a consistent rate of charge across time. Next, we will use varying-current variables for the model.

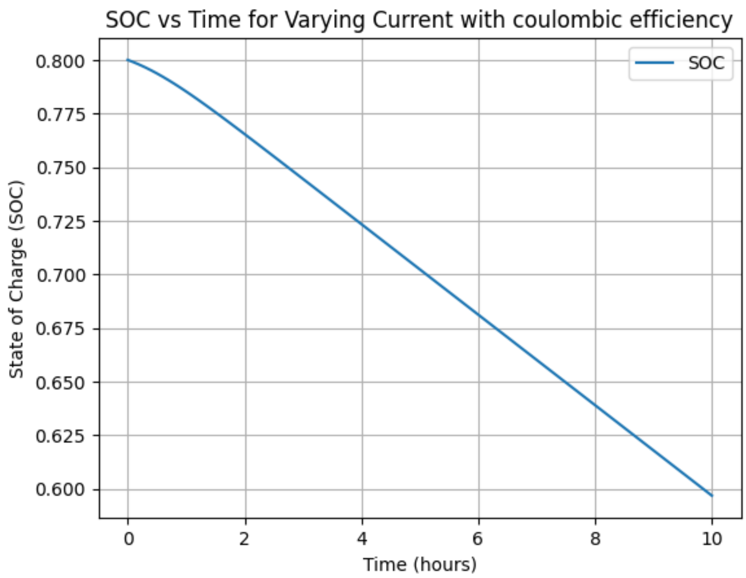

Figure 3: Discharge Profile of a Battery: State of Charge (SOC) Depletion Over Time when $I(t) = \tanh(t) + 1$ (Amps)"

The graph depicts how a battery's State of Charge (SOC) decreases over time when exposed to a variable current defined by $I(t) = \tanh(t) + 1$. Starting somewhat below 0.8, the SOC steadily drops, eventually reaching a little over 0.6 after 10 hours. In comparison to a situation with a fixed current, the gentler slope of this curve is due to the gradual drop of the current, which is consistent with the behaviour of the hyperbolic tangent function. Notably, the SOC does not dip below zero, indicating a range suitable for real-world battery usage. In the following section, we will construct our ECM by assembling its components systematically.

4.1 SOC to OCV

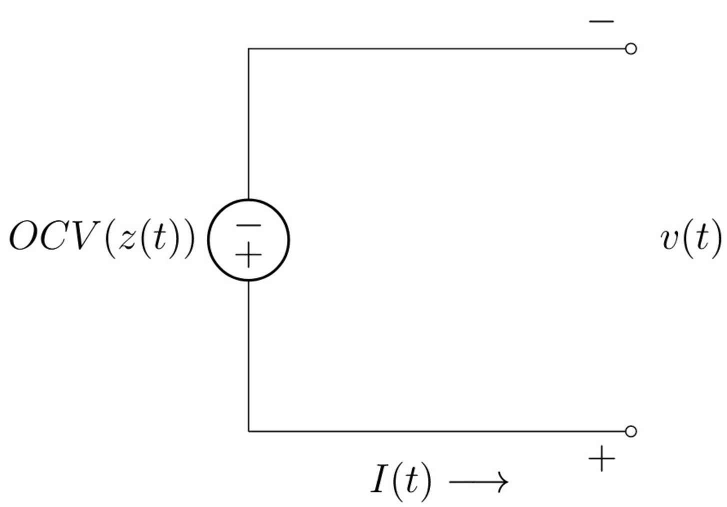

Figure 4: SOC to OCV equivalent circuit.

This is an equivalent circuit model that will include an ideal voltage source. Nevertheless, to account for the impacts of time-dependent input current, we will begin adding dynamic elements to the model. Initially, we want the model to represent the observation that, under loading conditions, the cell's terminal voltage falls below the OCV value and rises over the OCV value during charging. The regulated voltage source can be connected in series with a resistor to partially explain this behavior.

- Resistance [R]: Internal resistances take into consideration elements such as current collector resistance, electrode-electrolyte interface resistance, and electrolyte resistance to represent the ohmic [Ω] losses within the battery.
- Voltage [V]: This indicates the electric potential difference, which governs the behavior of simpler electrical components and influences energy distribution and usage in systems such as batteries. It is critical for studying and creating efficient, dependable electrical devices.

From this it can be written as:

$$V_{OCV}(z(t)) = OCV(z(t)) \tag{22}$$

The purpose of this is to represent voltage in relation to the OCV, which is dependent on the state of charge $z(t)$.
Every model has pros and cons listed with it. Below, I will start to list these:

Advantages:

- Clarity: The model is straightforward, making it easier to understand and implement.
- Predictive power: This model can accurately anticipate, in an open circuit, the voltage for a specific state of charge.
- Effective in stationary conditions: It gives precise voltage estimates in situations when the battery is not under dynamic or changing load.

Disadvantages:

- No load consideration: The load conditions are not taken into consideration in this model.
- Overtime inaccuracy: The model might not properly capture battery changes.

Next, this will begin to develop a more advanced model that can accommodate this, which is the linear polarisation.

5 Linear Polarization

5.1 Equivalent series resistance (ESR)

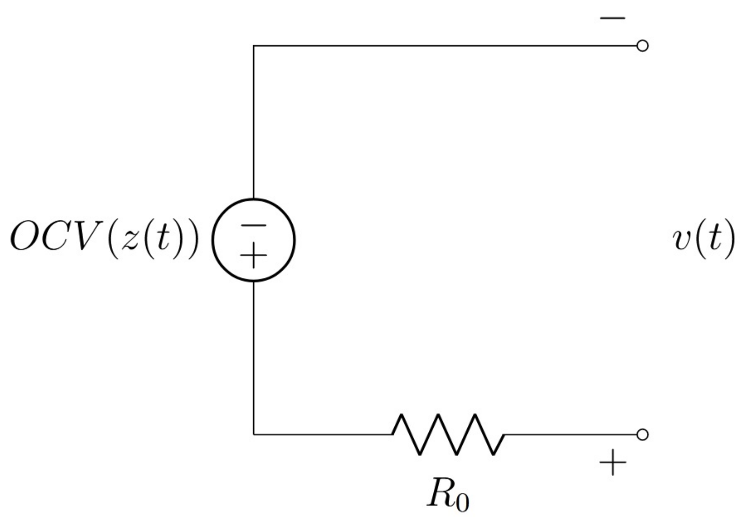

Figure 5: Equivalent Circuit for ESR model.

The so-called equivalent series resistance (ESR) of the cell is represented by the additional circuit component. The SOC equation is unchanged in the updated model. Nevertheless, in order to explain how to calculate the terminal voltage, including an additional equation in the model.

$$V_{R0}(t) = OCV(z(t)) - I(t)R_0 \tag{23}$$

Equation (23) shows that when

$$\text{When} \quad I(t) < 0, \quad V(t) > OCV(z(t)) \quad \Rightarrow \text{charging.}$$
$$\text{When} \quad I(t) > 0, V(t) < OCV(z(t)) \quad \Rightarrow \text{discharging.}$$

Each model is accompanied by a set of advantages and disadvantages. Below, I will start to list these:

Advantages:

- Simplicity: Simplifies the analysis of complex circuits by reducing components to their resistive elements, making calculations more straightforward.
- Linear behaviour: its ability to simplify complex circuit analyses, enabling more predictable and straightforward calculations.
- Single ODE: allows an ODE to be solved, allowing us to solve dynamic circuit problems efficiently.
- Low run time: it allows for rapid simulations and analyses, enhancing productivity in-circuit testing.

Disadvantages:

- Restricted accuracy: In dynamic environments, the model may oversimplify the behaviour of components across a range of operating conditions, resulting in inaccuracies.
- Linear behaviour for the battery: may not accurately reflect the nonlinear characteristics of battery performance under varied operational conditions.
- Ignores non-resistive properties: The primary emphasis is on resistive losses, potentially resulting in an inaccurate representation of other reactive elements.

In the following, I shall now delve into the Thevinen model, which has been enhanced.

6 Thevenin Model (1RC)

To represent the dynamic behavior of LiB by Thevenin model is used. incorporating a solitary resistor-capacitor (RC) pair alongside the fundamental components of an OCV source and a series resistor. The 1RC pair Thevenin model is particularly valued for its ability to balance simplicity with the accuracy needed for many practical applications.

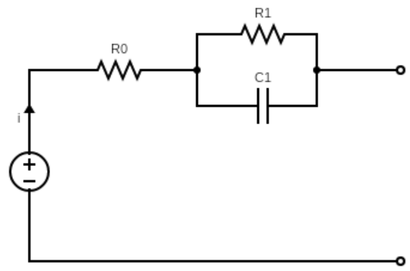

Figure 6: Thevenin 1RC circuit

- R0 : Ohmic resistance [Ω]
- R1 : Resistance due to chemical relations[Ω]
- C1 : Capacitance to represent the dynamic behavior of the cell.

$$V_t = OCV(z(t)) - V_{C_1}(t) - I(t)R_0 \tag{24}$$

As I_{R_1} is unknown , this can rewritten as:

$$I_{C_1}(t) = C_1 \frac{dV_{C_1}(t)}{dt}$$

To find I_{R_1} we can use Kirchoff's current law:

$$I_{R_1}(t) + C_1 \frac{dV_{C_1}(t)}{dt} = I(t)$$

Using the relation between resistance and current-voltage:

$$V_{C_1}(t) = I_{R_1}(t)R_1 \tag{25}$$

$$I_{R_1}(t) + C_1R_1 \frac{dI_{R_1}(t)}{dt} = I(t) \tag{26}$$

$$\frac{dI_{R_1}(t)}{dt} = \frac{I(t)}{C_1R_1} - \frac{I_{R_1}(t)}{C_1R_1} \tag{27}$$

Along with the above equation, I also solve the equation for $z(t)$. Hence, our closed model for 1RC pair with appropriate initial conditions is

$$\boxed{\begin{aligned} &\frac{dz(t)}{dt} = -\frac{I(t)\eta(t)}{Q}, \\ &\frac{dI_{R_1}(t)}{dt} = \frac{I(t)}{C_1R_1} - \frac{I_{R_1}(t)}{C_1R_1}, \\ &z|_{t=t_0} = z_0, \quad I_{R_1}|_{t=t_0} = I^0_{R_1}, \\ &V_{R_1}(t) = OCV(z(t)) - I_{R_1}(t)R_1 - I(t)R_0, \end{aligned}} \tag{28}$$

Previously, I only needed to solve one ODE, but now I have two ODEs that can be solved analytically.

Analytical solution of equation (27) Initial conditions are imposed on the equation such that I_{R_1} is equal to $I_{R_1}^0$ at time t=0, whereas in our model it is $I_{R_0} = 0.345$. For our unknown parameters, such as C_1 and R_1, firstly, will let $C_1 = 8898$ as our initial guess and $R_1 = 0.000333$ as our other initial guess. I selected these values based on [25, 26]. With R_1, we will use optimisation so that it is more accurate to our plot, Where R_1 optimal will give us 0.296.

Given the equation : $\frac{dI_{R_1}(t)}{dt} = \frac{I(t)}{C_1R_1} - \frac{I_{R_1}(t)}{C_1R_1}$ we have to find what $I_{R_1}(t)$ is. Given the differential equation:

$$\frac{dI_{R_1}(t)}{dt} + p(t)I_{R_1}(t) = q(t)$$

where $p(t) = \frac{1}{R_1C_1}$ and $q(t) = \frac{1}{C_1R_1}I(t)$. First, identify the integrating factor:

$$\mu(t) = e^{\int p(t)\,dt} = e^{\int \frac{1}{R_1C_1}\,dt} = e^{\frac{t}{R_1C_1}}$$

Multiplying both sides of the differential equation by the integrating factor:

$$e^{\frac{t}{R_1C_1}}\frac{dI_{R_1}(t)}{dt} + e^{\frac{t}{R_1C_1}} \cdot \frac{1}{R_1C_1}I_{R_1}(t) = e^{\frac{t}{R_1C_1}} \cdot \frac{1}{C_1R_1}I(t)$$

This simplifies to:

$$\frac{d}{dt}\left(e^{\frac{t}{R_1C_1}}I_{R_1}(t)\right) = \frac{e^{\frac{t}{R_1C_1}}}{C_1R_1}I(t)$$

Now integrate both sides from t_0 to t:

$$e^{\frac{t}{R_1C_1}}I_{R_1}(t) - e^{\frac{t_0}{R_1C_1}}I_{R_1}(t_0) = \int_{t_0}^{t}\frac{e^{\frac{t}{R_1C_1}}}{C_1R_1}I(t)\,dt$$

Solving for $I_{R_1}(t)$:

$$e^{\frac{t}{R_1C_1}}I_{R_1}(t) = e^{\frac{t_0}{R_1C_1}}I_{R_1}(t_0) + \int_{t_0}^{t}\frac{e^{\frac{t}{R_1C_1}}}{C_1R_1}I(t)\,dt$$

Finally, isolate the $I_{R_1}(t)$:

$$I_{R_1}(t) = e^{-\frac{t}{R_1C_1}}\left(e^{\frac{t_0}{R_1C_1}}I_{R_1}(t_0) + \int_{t_0}^{t}\frac{e^{\frac{t}{R_1C_1}}}{C_1R_1}I(t)\,dt\right)$$

This is the solution with the integral bounds from t_0 to t. This model offers the following advantages and disadvantages:

Advantages:

- First-order equation: Enable straightforward and rapid analytical solutions
- low complexity: It makes comprehension, application, and computation faster.

Disdvantages:

- Varying parameters: That may reduce its ability to accurately depict changing real-world situations.

7 PNGV Model

The PNGV model stands for the "Partnership for a New Generation of Vehicles" model. It is a type of battery model developed under the PNGV program. The PNGV battery model has been purposefully developed to simulate and forecast the performance of batteries across a range of operational circumstances, with a particular emphasis on hybrid and electric vehicles. This model falls into the category of ECMs and is often used to evaluate and analyze the performance and life cycle of vehicular batteries. This model accounts for variation in temperature for voltage and SOC.

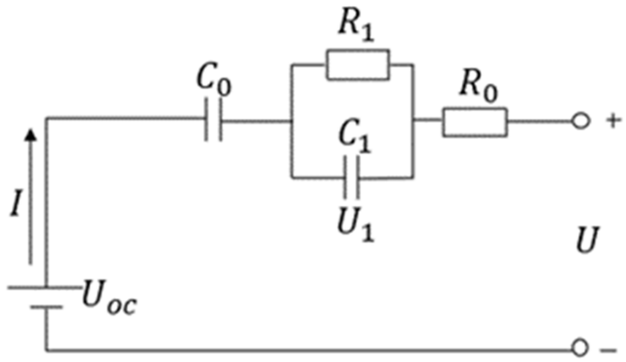

Figure 7: PNGV circuit model [27]

Remodeling the previous equation following the PNGV standard:

$$\boxed{\begin{aligned}
&\frac{dz(t)}{dt} = -\frac{I(t)\eta(t)}{Q},\\
&\frac{dI_{R_1}(t)}{dt} = \frac{I(t)}{C_1R_1} - \frac{I_{R_1}(t)}{C_1R_1},\\
&\frac{dV_{C_0}}{dt} = OCV(z(t)) - I(t),\\
&z|_{t=t_0} = z_0, \quad I_{R_1}|_{t=t_0} = I^0_{R_1}, \quad V_{C_0}|_{t=t_0} = V^0_{C_0},\\
&V_t(t) = OCV(z(t)) - I_{R_1}(t)R_1 - I(t)R_0 - V_{C_0}
\end{aligned}} \tag{29}$$

Where :

$$\int_{t_0}^{t} \frac{dV_{C_0}}{dt}\, dt = \int_{t_0}^{t} \mathrm{OCV}(z(t))I(t)\, dt$$

The left-hand side simplifies to:

$$V_{C_0}(t) - V_{C_0}(t_0) = \int_{t_0}^{t} \mathrm{OCV}(z(t))I(t)\, dt$$

Solving for $V_{C_0}(t)$:

$$V_{C_0}(t) = V_{C_0}(t_0) + \int_{t_0}^{t} \mathrm{OCV}(z(t))I(t)\, dt$$

Having greater accuracy than the others, this model will offer advantages as well as disadvantages.

Advantages:

- Additional capacitor: This represents voltage changes in circuits.
- Low runtime: As a result of its simplified structure, reduced computational demand, and efficient parameterization in comparison to more complex battery models

Disdvantages:

- Additional capacitors: This can cause certain inaccuracies in voltage.
- Charge/Discharge: This model does not account for self discharge behaviour.

- Accurate sensitivity: Is exceedingly susceptible to its parameters. Small errors in parameter estimation can lead to significant deviations in the output.

In the following , I investigate several numerical methods implemented for the models built previously.

8 Numerical Methods

In this section, we discuss various numerical methods applied to the models developed in previously, beginning with essential model parameters such as the initial SOC and OCV of the cell. For validation purposes, we utilised Dandeliion, where we collected 'Total Voltage' and 'Total Current' data for different C-rate. This data is crucial as it allows us to compare the results of our model at each C-rate, thereby validating the accuracy and reliability of our models. By thoroughly comparing our model results with the Dandeliion data, we aim to establish the robustness and precision of the developed models.

9 Finding Open-circuit voltage (OCV) [11, 10]

In order to compare our model, we require experimental OCV. To do this, we will start by using data from a discharge at a rate of $C/200$ - C-rate. I utilise the Dandeliion Kokam 7.5Ah pouch cell [12, 11] to obtain voltage and current data at $\frac{C}{200}$ - C-rate. We will use this voltage as an experiment OCV throughout the study. We fit the experimental to the OCV curve using interpolation.

10 Interpolation

Using the definition in [19] interpolation is a mathematical method of predicting new points or values from a discrete set of known data points. The goal is to create a function that smoothly fits these known points, allowing for the estimation of values at intermediate positions. This is used in our program as `scipy.interpolate`, which allows us to achieve the desired function. Linear interpolation is one of the simplest methods used, which utilizes two data points, for instance, (x_a, y_a) and (x_b, y_b), and the interpolant is provided by:

$$f(x) = y_a + \frac{(y_b - y_a)}{x_b - x_a} \times (x - x_a) \tag{30}$$

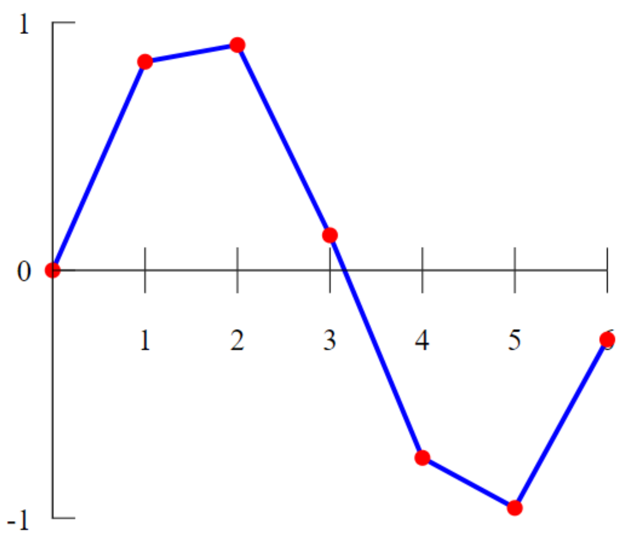

Figure 8: Example of linear interpolation [19]

11 Cubic interpolation[20]

Cubic interpolation is a method of estimating new data points inside a certain range by using cubic polynomials, which are polynomial functions of degree three. It constructs a smooth, continuous curve that passes through the given data points by fitting a cubic polynomial between each pair of points.
This is the reason we can now determine a cell's voltage of:

$$V = OCV(z(t)) \tag{31}$$

as well as the ESR model:

$$V = OCV(z(t)) - I(t)R_0 \tag{32}$$

same thing we solve for z(t) we now have a new parameter R_0, which is ohmic resistance in the model. To find this parameter, we use optimisation.

12 BFGS Optimization Algorithm

Following from [21] The BFGS (Broyden-Fletcher-Goldfarb-Shanno) optimisation algorithm is a technique employed to locate the local maximum or minimum of a function. It is an iterative technique for solving unconstrained, nonlinear optimisation problems. BFGS is a member of the quasi-Newton methods, a class of algorithms that estimate the Hessian matrix of second derivatives (which characterises the curvature of the optimised function) without the requirement for direct computation. The algorithm updates an estimate of the inverse Hessian matrix at each step using rank-two updates specified by gradient evaluations. By doing so, BFGS adjusts the direction and step size of the search to more efficiently converge towards the optimum with fewer function evaluations compared to other optimisation methods. The use of BFGS for estimating optimal R_0 is advantageous since it is highly efficient in dealing with intricate, non-linear optimisation issues that may involve extensive parameter spaces, a common occurrence in battery modelling scenarios.

The code optimises utilising mean square error, which is calculating the mean of the squared discrepancies between the predicted and actual values.

$$\min_{R_0} \sum_{i=1}^{n} (\tilde{V}(t_i) - V(t_i, R_0))^2 \tag{33}$$

$$\text{When: } V \quad \Rightarrow \text{Solution of the model} \tag{34}$$

$$\text{When: } \tilde{V} \quad \Rightarrow \text{Experiment data} \tag{35}$$

We apply the same optimisation method to R_1 while using the optimised R_0 while using, as stated previously, the initial guess $R_1 = 0.000333$.

$$\min_{R_1} \sum_{i=1}^{n} (\tilde{V}(t_i) - V(t_i, R_1))^2 \tag{36}$$

$$\text{When: } V \quad \Rightarrow \text{Solution of the model} \tag{37}$$

$$\text{When: } \tilde{V} \quad \Rightarrow \text{Experiment data} \tag{38}$$

13 Charge Cycle

A charge cycle is the process of charging a rechargeable battery from discharged to completely charged and then discharging it back to its original state. Each cycle has an impact on the battery's capacity, with some degradation over time [23]. We start to apply this model by using this method of code:

```
time_values = np.linspace(0,4*3600,10000)
def I_of_(t):
    current = np.zeros_like(t)
    current[t <= 3600 ] = 0.15625   # First hour
    current[t > 3600 ] = -0.15625   # Second hour
    current[t > 3600*2 ] = 0.15625   # Third hour
    current[t > 3600*3 ] = -0.15625   # Fourth hour
    current[t > 3600*4 ] = 0.15625   # Beyond four hours

    return current
```

14 Battery Capacity

Battery capacity is the quantity of power required by electric charges to carry out certain operations. The rate at which electrical energy is consumed is known as electric power and is measured in watts [24]. Using Kirchhoff's law, we can simply calculate the power in an electric circuit. The formula for calculating electrical power is as follows:

$$P = IV \tag{39}$$

With this, we can now calculate the power that's required in our experiment.

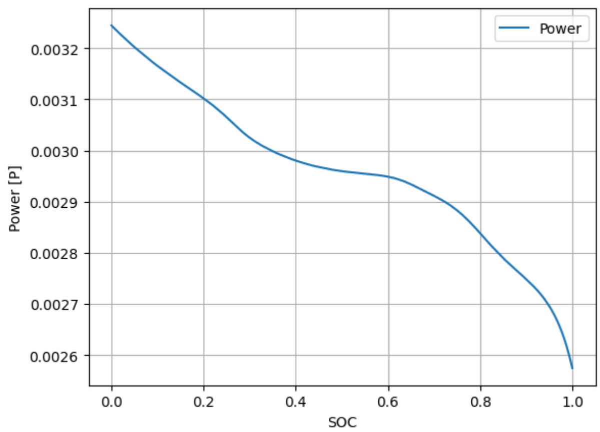

Figure 9: Experimental data power

The power output exhibits a gradual decrease as the SOC progresses from 0 (indicating complete discharge) to 1 (confirming complete charging). Initially, the power output is relatively high at low SOC values, but it decreases as the SOC increases. The plot emphasises the dynamic behaviour of the battery's power output, its SOC, which is important for optimising battery performance. Our model is ready for testing, and in the following few plots, we will present all the necessary parameters. Here I'll be going through the results that I've managed to gain with each model.

14.1 Dandeliion Kokam 7.5Ah pouch cell Results [12]

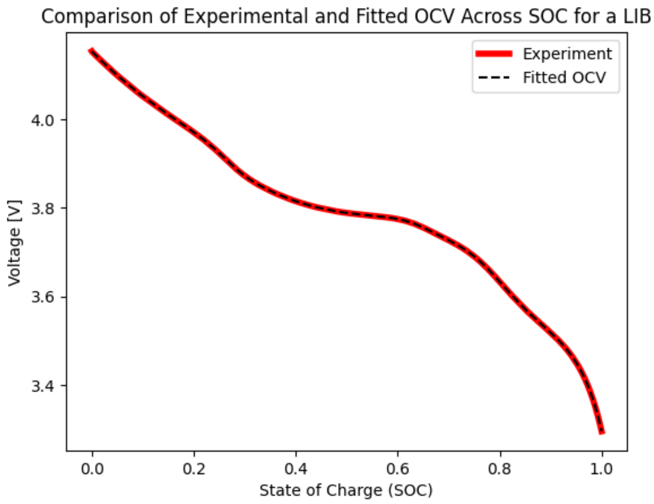

Figure 10: Experimental data and Fitted OCV

Figure 10 displays an experimental OCV that is accurately matched by the interpolated fitted OCV.

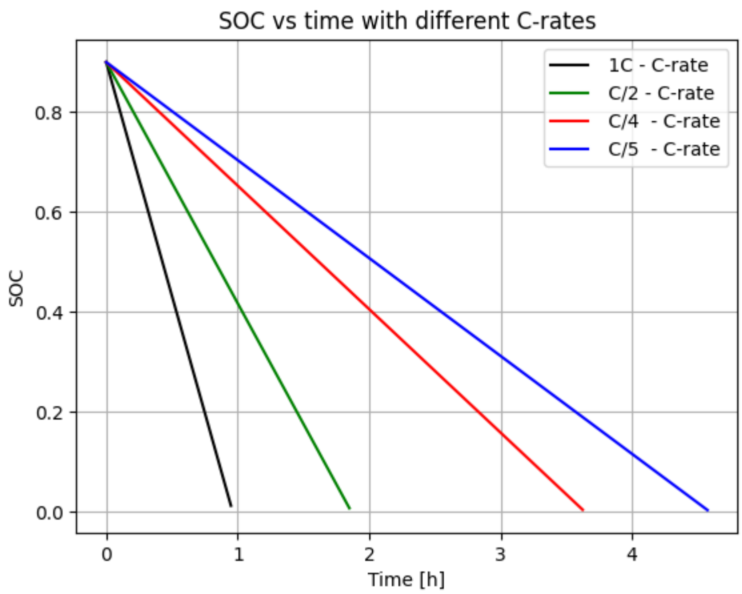

Figure 11: SOC against Time with different C-rates.

In Figure (11), We can see that a discharge of 1C - C-rate means that the battery will be completely depleted in one hour. A discharge of $\frac{C}{2}$ C-rate would take two hours, and so on. We can see that in the graph, the higher the C-rates, the faster the depletion of the battery's SOC, indicating the battery running out of charge more quickly. However, on the contrary, the lower the C-rate, the slower the discharge, meaning the battery would last longer, as seen in the blue line $\frac{C}{5}$ C-rate. The SOC diminishes in a linear manner as time progresses for each C-rate, indicating a direct correlation between the discharge rate and the reduction of SOC over time.

Revisiting Equation (23), we commence the application of distinct C-rates to initiate the equation. Through the employment of interpolation techniques alongside the BFGS optimization algorithm, we establish both an initial estimate and an optimized value for the parameter R_0. This process enables us to discern the variance between the preliminary and refined estimates of R_0. Subsequently, a comparative analysis is undertaken to elucidate the contrasts and similarities elicited by these different approaches.

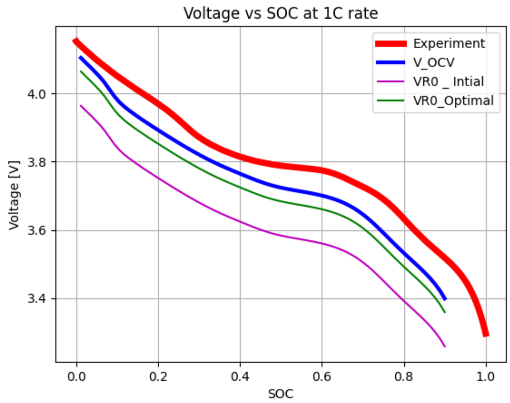

Figure 12: 1C-rate

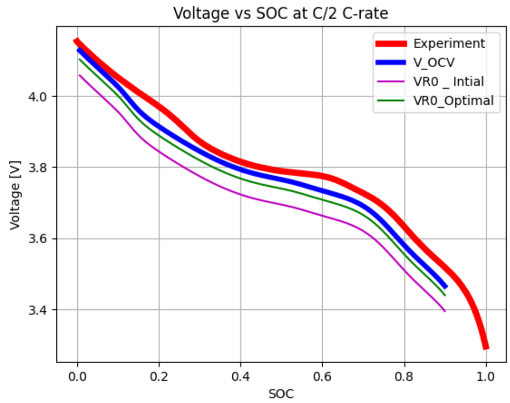

Figure 13: C/2 C-rate

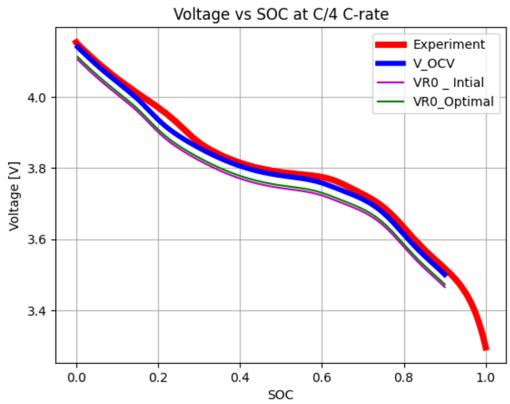

Figure 14: C/4 C-rate

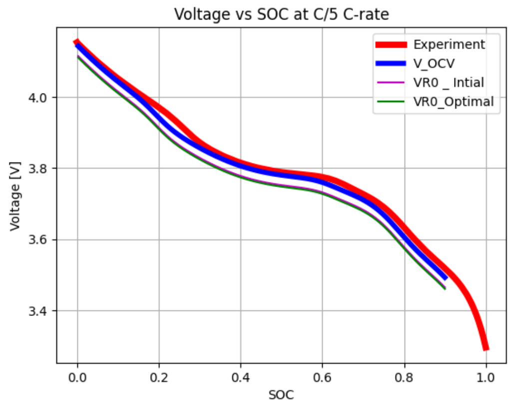

Figure 15: C/5 C-rate

Beginning with the 1C rate, which represents a rapid charging scenario, we utilize simplified models such as the ECM. This particular model is acknowledged to be less accurate compared to more complex ones, which aligns with expectations. It is observable that at 1C, both the experimental and the fitted OCV experience a rapid decline in SOC in contrast to other models, where the depletion occurs at a more uniform rate.

Additionally, across all models, it is evident that our optimal V_{R_0} aligns better with the experimental data, in contrast to the initial V_{R_0}. It's evident that as the C-rate increases, the quality of the plot improves. This is because a longer C-rate indicates a slower discharge or charge rate relative to the battery's capacity, allowing for more accurate and stable measurements.

The experimental findings clearly show a more pronounced decrease in voltage at the faster $\frac{C}{2}$ C-rate pace compared to the slower $\frac{C}{4}$ C-rate. Next, we will begin utilising data obtained from a gradual discharge at a rate of 1C in order to obtain a precise measurement of the capacity. We utilise the Dandeliion LG M50 21700 5Ah battery [10] to obtain voltage and current data and we will refer to them as experiment. We will now proceed to apply the identical procedures used on the Kokam 7.5Ah pouch cell to the LG M50 21700 5Ah battery.

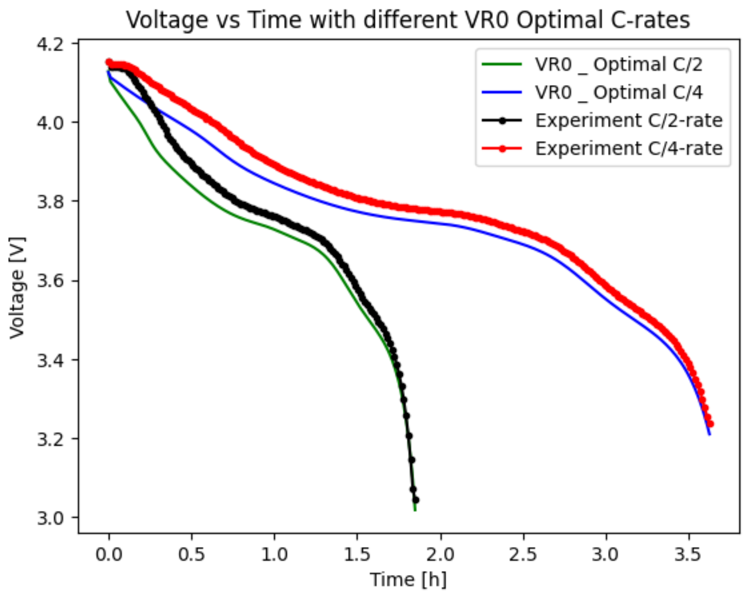

Figure 16: R_0 initial = 0.9 and R_0 optimal = 0.7

14.2 Dandeliion LG M50 21700 5Ah battery Results

The 'flat top' of the battery refers to a where the voltage is always consistently stable, even at High SOC levels. This indicates that the battery is fully charged or very close to being fully charged.

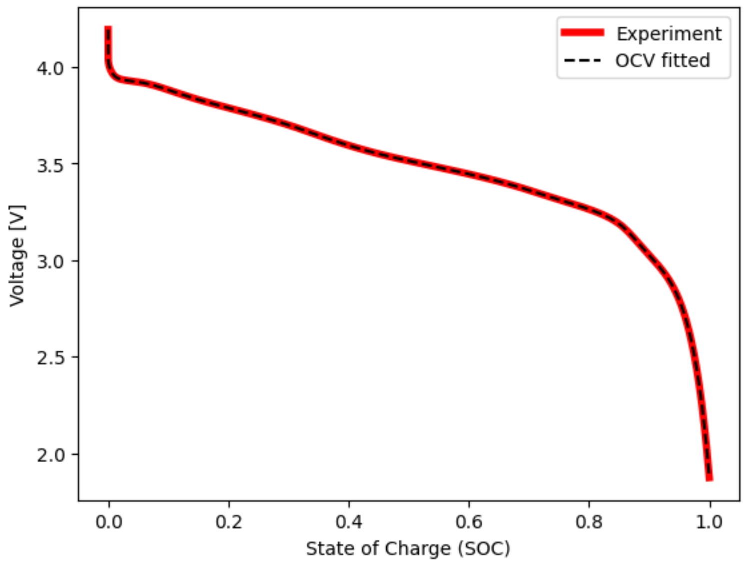

Figure 17: Experimental data and Fitted OCV

As the battery discharges, the voltage gradually decreases and then drops more sharply as the SOC decreases, a common trait in LiB due to the depletion of available energy. The OCV fitted curve closely mirrors the experimental data, suggesting that the mathematical model used for the OCV provides an accurate representation of the battery's behavior without continuous experimental measurement.

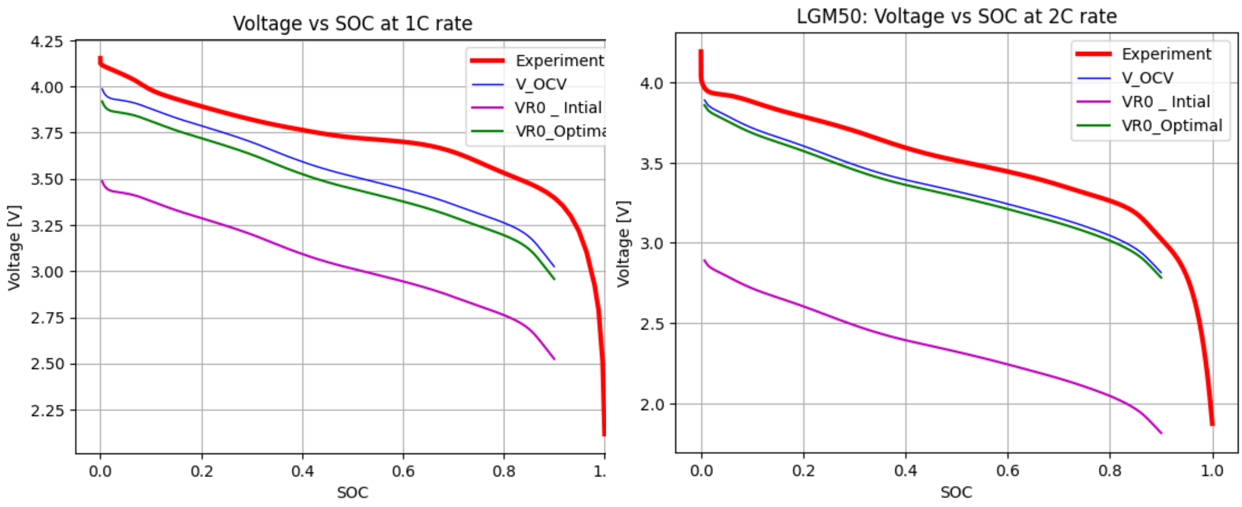

Figure 18: Plots of Voltage vs SOC at different C-rates

A discharge rate of 1C indicates that the battery would be completely drained within one hour. This is demonstrated by the black line dropping steadily over time. The 2C rate, represented by the green line, suggests a faster depletion, fully discharging the battery in just half an hour.

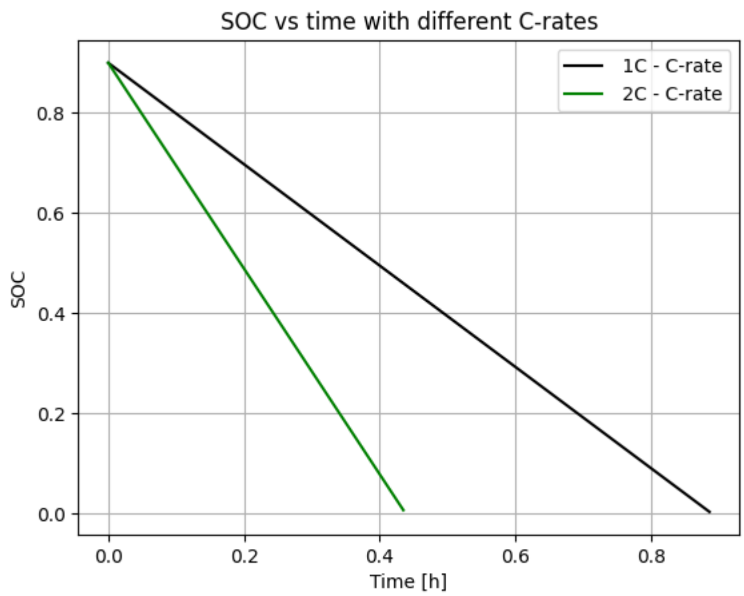

Figure 19: SOC against Time with different C-rates

This steeper decline demonstrates that as the discharge rate doubles, the time required for the battery to exhaust its charge is halved, highlighting the inverse relationship between discharge rates and discharge duration.
Both plots display a decreasing voltage as the state of charge (SOC) decreases, suggesting a depletion of energy. The 1C rate graph demonstrates a more gradual voltage decline, while the 2C rate graph shows a steeper drop, reflecting the faster discharge. Although both rates exhibit a similar pattern, the voltage falls more swiftly at the higher 2C rate due to the more rapid energy discharge.
At the 2C rate, it is evident that the optimal model approaches the OCV. This observation indicates that as the C-rate increases, meaning the battery is charged or discharged more quickly, the model's predictions align more closely with the experimental data.

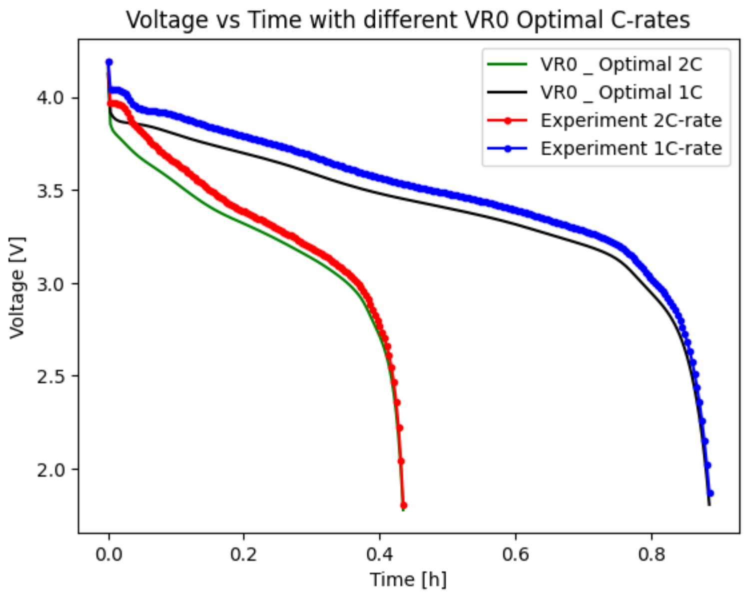

Figure 20: Voltage against Time with different V_{R_0} optimal C-rates

The primary objective of the V_{R0} models is to closely align with the experimental data. The voltage decreases more rapidly for the 2C rate, evident from the steeper slope, meaning the battery depletes faster at this rate. The models seem to track the experimental discharge curves well, indicating they provide a reliable representation of the battery's behavior under these specific discharge conditions.

15 Thevenin (1RC) results

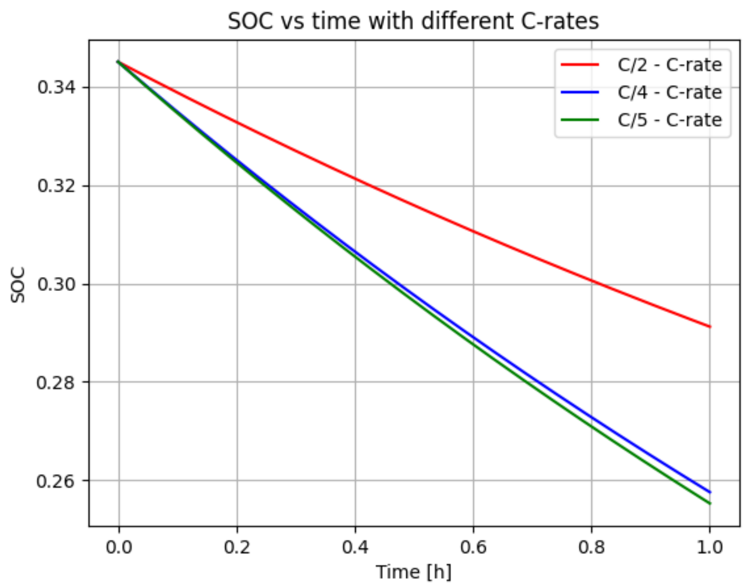

Figure 21: SOC against time with different C-rates

The battery maintains a higher SOC for the same duration, as indicated by the plot. The red line represents the fastest discharge rate ($\frac{C}{2}$), resulting in the quickest decrease in SOC. The blue line ($\frac{C}{4}$) and the green line ($\frac{C}{5}$) represent slower discharge rates, showing less steep declines in SOC over the hour.

The provided plots illustrate the voltage characteristics of a LiB about its SOC as the discharge rate changes. The data showcases experimental results alongside predictions from V_{OCV} and a 1RC

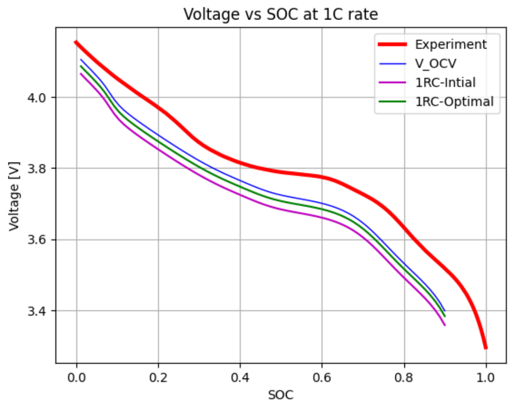

Figure 22: 1C-rate

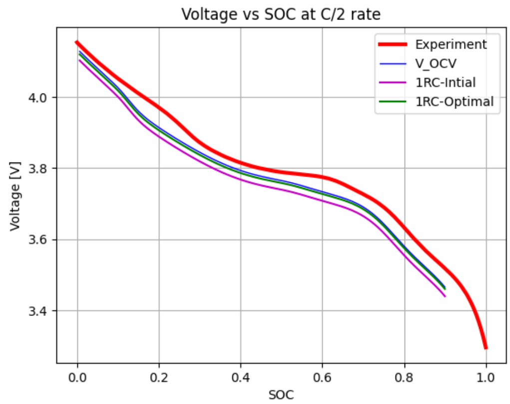

Figure 23: C/2 C-rate

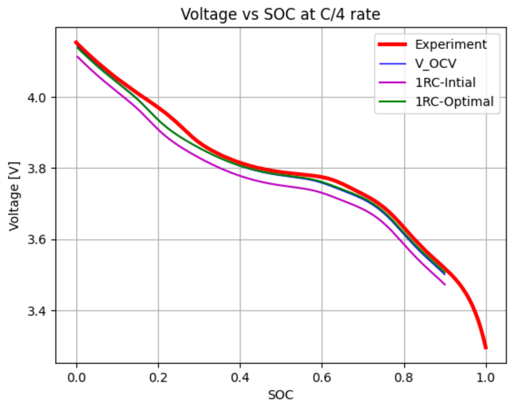

Figure 24: C/4 C-rate

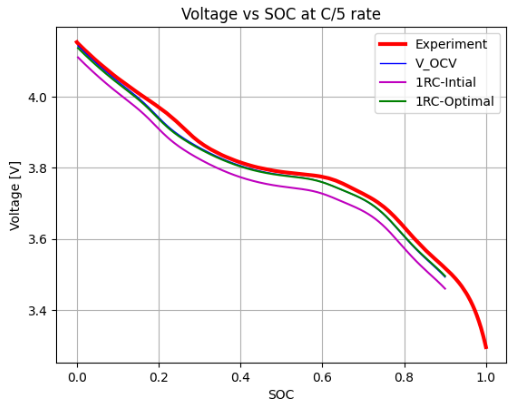

Figure 25: C/5 C-rate

pair model. As the discharge rate decreases from 1C to $\frac{C}{5}$, we observe that the 1RC-optimal model increasingly aligns with the experimental data. This trend is due to the reduced stress and more stable conditions at lower C-rates, allowing the model to better capture the battery's behaviour. The 1RC-initial model, with its initial parameter settings, shows greater deviation, particularly at higher rates, indicating that parameter optimisation is crucial for accurate predictions. Overall, the 1RC-optimal model demonstrates its robustness and accuracy, especially under less intense operational stresses.

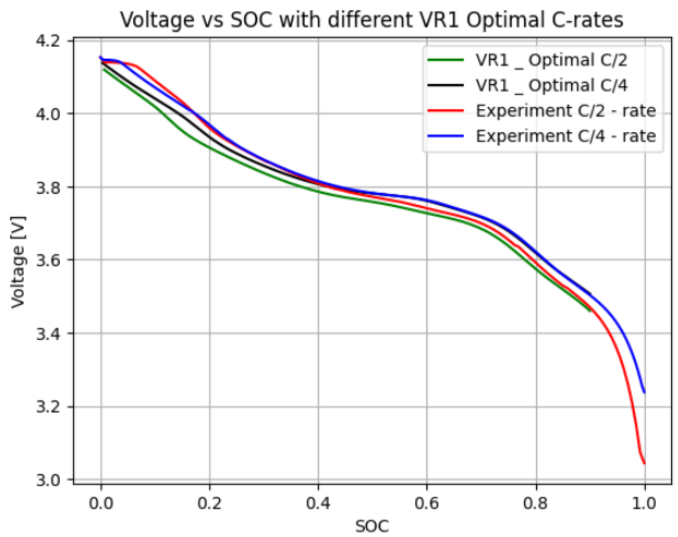

Figure 26: Voltage against SOC with different RC1 optimal C-rates

The voltage decline of a battery over time is illustrated in the plot, with experimental data being compared to predictions generated by the V_{R_1}-optimal model for two distinct discharge rates ($\frac{C}{2}$ and

$\frac{C}{4}$). The V_{R_1}-optimal models both start close to their corresponding experimental lines but exhibit some deviations as the discharge progresses. The experimental data, shown in red for $\frac{C}{2}$ and blue for $\frac{C}{4}$, indicates that the battery's voltage decline is more pronounced at the higher discharge rate ($\frac{C}{2}$). This illustrates the impact of discharge rate on battery voltage behaviour and highlights the V_{R1}-optimal model's general capability.

16 PNGV results

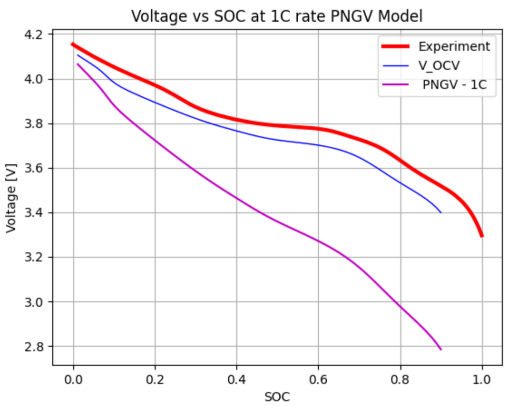

Figure 27: 1C-rate

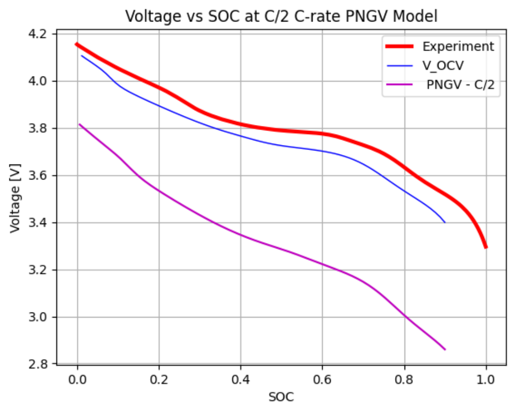

Figure 28: C/2 C-rate

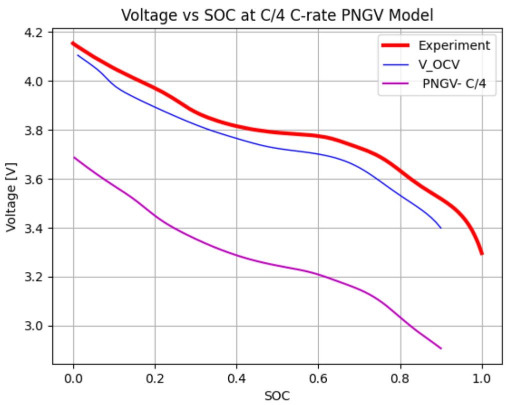

Figure 29: C/4 C-rate

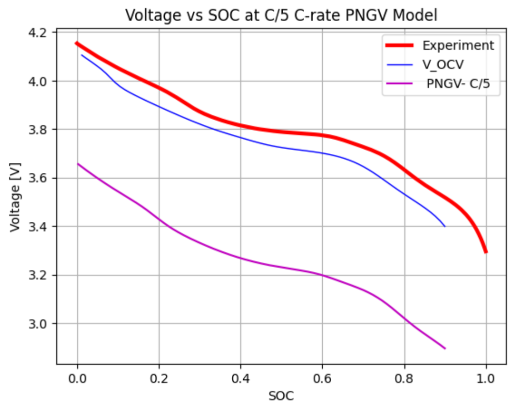

Figure 30: C/5 C-rate

The plots depict the voltage versus SOC for LiB at various discharge rates (1C, $\frac{C}{2}$, and $\frac{C}{4}$), comparing experimental data, OCV, and the PNGV model. At the $1C$ rate, the PNGV model deviates significantly from the experimental data, especially at lower SOC values, indicating a need for parameter adjustments. As the discharge rate decreases to $\frac{C}{2}$ and $\frac{C}{4}$, the model aligns more closely with the experimental data, although some discrepancies persist. This suggests that the PNGV model is more accurate under lower stress conditions but requires further refinement for higher rates. The OCV model consistently provides a theoretical baseline across all plots.

17 Charge Cycle results

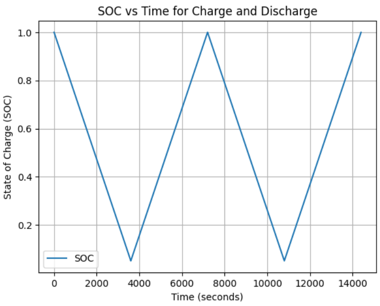

Figure 31: Charge/Discharge rates

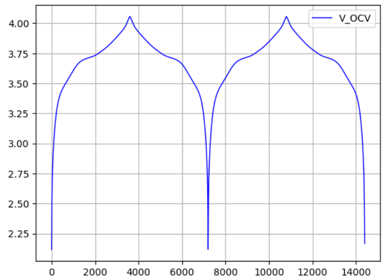

Figure 32: Voltage Discharge/Charge

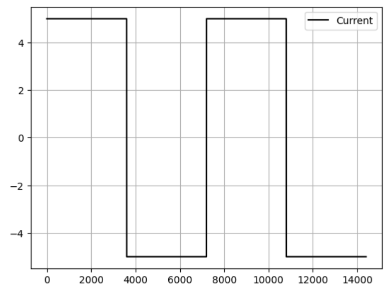

Figure 33: Current rates

The behaviour of a LiB throughout charge and discharge cycles is depicted in the three graphs. The first plot shows the SOC oscillating between fully charged and fully discharged states in a saw-tooth pattern over time, indicating consistent charging and discharging cycles.

The current in the second plot exhibits a square wave pattern characterised by positive and negative oscillations; this corresponds to the constant current that is supplied throughout the charging and discharging stages.

The OCV, which increases during charging and decreases during discharging by the SOC variations, is depicted in the third plot. The performance and efficacy of the battery under controlled cycling conditions are collectively illustrated in these plots, which offer significant insights that can be utilised to optimise battery management.

18 Conclusion

This study involved the development and evaluation of various equivalent circuit models for lithium-ion batteries. These models ranged from a basic state of charge to a voltage model and included more complex networks with multiple resistors and capacitors. The specific models used in this study were: open circuit voltage, state of charge, linear polarisation, Thevnin model, PNGV, and charge cycle. These models were implemented in Python, solving the governing ordinary differential equations to obtain the state of charge and voltage response. The dandeliion solver was used to extract experimental voltage data from a Kokam 5A pouch cell and an LG M50 cylinderical cell. The data was collected at several C-rates (1C, $\frac{C}{2}$, $\frac{C}{4}$, $\frac{C}{5}$, $\frac{C}{200}$) and preprocessed using interpolation techniques. An optimisation algorithm was utilised to calculate the most suitable parameter values for each model by minimising the discrepancy between simulated and experimental voltages.

The comparison of generated voltage outputs with experimental data across a range of C-rates led us to the conclusion that the models are more accurate the longer the duration. Specifically, the models showed significant improvements in accuracy as the runtime grew and the discharge rates fell. For instance, at lower C-rates, such as C/4 and C/5, the models' predictions and the experimental findings agreed closely, highlighting the models' increased accuracy and dependability over extended periods of time. Furthermore, experimental setup constraints in dandeliion prevented us from obtaining experimental data when we tried to use charge cycles for additional validation. This restriction kept us from investigating the impact of charge cycles on the models.

This systematic model comparison offers advice on choosing suitable equivalent circuit models for lithium-ion batteries. Future work can explore further model refinements and integration with thermal effects.

19 Future Work

This presents potential paths for future research to expand upon the discoveries of this study. Although our current work offers valuable insights into the performance of equivalent circuit models for lithium-ion batteries, there are several aspects that require more examination to improve the understanding and implementation of these models, particularly in temperature effects.

Temperature has a crucial role in determining how batteries work, how safe they are, and how long they last. Including temperature in modelling efforts can enhance our understanding of battery behaviour in a more comprehensive manner. The current analysis focuses on isothermal conditions. Incorporating temperature dependencies in the model parameters would enable simulating battery behaviour across a wider range of thermal operating environments.

By addressing this future research direction, the equivalent circuit modelling paradigm can evolve into a more comprehensive tool for optimising battery performance, life cycle, safety, and cost in a wide range of applications.

Acknowledgements

First and foremost, I would like to sincerely thank my supervisor, Smita Sahu, for her essential mentorship, assistance, and motivation during the duration of this project. Her expertise and insights have been instrumental in shaping this work. I am deeply appreciative of the teachers and staff in School of Mathematics and Physics at the University of Portsmouth for creating a superb academic setting and offering resources that greatly aided my study.

I am deeply indebted to my family and friends for their unwavering support and encouragement throughout my academic journey. In particular, I wish to honor the memory of my late parent, Kay Fathealdeen, whose love, wisdom, and guidance have been a source of inspiration and strength throughout this journey. Their enduring presence in my heart has motivated me to persevere, and this work is dedicated to their memory. Though their absence is deeply felt, their spirit continues to guide me.

I would want to express my sincere gratitude to my surviving parent, Tariq Fathealdeen, as well as my siblings, for their continuous support and understanding. Their patience, encouragement, and belief in me have been indispensable throughout this journey.

References

[1] What is lithium-ion battery how do lithium-ion batteries work ,19 November 2021.

[2] Kirchhoff's circuit laws." Wikipedia: The Free Encyclopedia. Wikimedia Foundation, Inc. 22 April 2024. Web.

[3] Kirchhoff, G. (1847). "On the passage of an electric current through a plane and through areas," Annals of Physics, 72(5), 497-508.

[4] Gregory Plett. (2015). Battery Management Systems, Volume I: Battery Modeling: Power Engineering and Power El September 30, 2015.

[5] Barletta, G., DiPrima, P., and Papurello, D. (Year). Thevenin's Battery Model Parameter Estimation Based on Simulink.

[6] I. Korotkin, S. Sahu, S. E. J. O'Kane, G. Richardson, J. M. Foster, "DandeLiion v1: An extremely fast solver for the Newman model of lithium-ion battery (dis)charge", Journal of The Electrochemical Society, Volume 168, Number 6, 060544 (2021).

[7] M. Doyle, J. Newman, A. S. Gozdz, C. N. Schmutz, and J.-M. Tarascon, *Comparison of modeling predictions with experimental data from plastic lithium ion cells*, Journal of the Electrochemical Society, **143**, (1996), pp. 1890–1903.

[8] M. Doyle, T. F. Fuller, and J. Newman, *Modeling of galvanostatic charge and discharge of the lithium/polymer/insertion cell*, Journal of the Electrochemical Society, **140**, (1993), pp. 1526–1533.

[9] T. F. Fuller, M. Doyle, and J. Newman, *Simulation and optimization of the dual lithium ion insertion cell*, Journal of the Electrochemical Society, **141**, (1994), pp. 1–10.

[10] www.dandeliion.com, DandeLiion legacy version 2020.

[11] Simulation link for OCV curve Job "Gr/NMC single cell (Ecker et al.) C/200 https://simulation.dandeliion.com/legacy/simulation/?id=46270a00-d806-41f5-b4bb-5dcaf45fc18b

[12] Ecker, M., Tran, T. K. D., Dechent, P., Käbitz, S., Warnecke, A., and Sauer, D. U. (2015). Parameterization of a Physico-Chemical Model of a Lithium-Ion Battery: I. Determination of Parameters. Journal of The Electrochemical Society, 162(9), A1836. DOI: 10.1149/2.0551509jes

[13] WBU-204: How do Lithium Batteries Work? ,22 Feburary 2022.

[14] Crompton, Thomas Roy(2000). Battery reference book.

[15] Murashko, Kirill (2016). Thermal modelling of commercial lithium-ion batteries.10.13140/RG.2.1.3930.0723

[16] Schipper, Florian and Nayak, Prasant Kumar and Erickson, Evan M and Amalraj, S Francis and Srur-Lavi, Onit and Penki, Tirupathi Rao and Talianker, Michael and Grinblat, Judith and Sclar, Hadar and Breuer, Ortal (2017).Study of cathode materials for lithium-ion batteries: Recent progress and new challenges, Inorganics. v.5 , p.32.

[17] Parameterization of a Physico-Chemical Model of a Lithium-Ion Battery: Determination of Parameters Madeleine Ecker.29 June 2015.

[18] Britannica, "electric circuit" , 28 March 2024.

[19] Wikipedia contributors (2024), "Interpolation — Wikipedia, The Free Encyclopedia" .

[20] Qingkai Kong, Timmy Siauw, Alexandre, Python Programming and Numerical Methods, 27 November 2020.

[21] Megha Garg. BFGS Optimization Algorithm, Shiksha Online. 9 feburary 2023.

[22] Wikipedia contributors (2024), "Euler method — Wikipedia, The Free Encyclopedia", 27 November 2020.

[23] Wikipedia contributors (2023),"Charge cycle — Wikipedia, The Free Encyclopedia"

[24] Anker (Jun 28, 2023), Understanding Battery Capacity: A Comprehensive Guide

[25] Giulio Barletta, Piera DiPrima, and Davide Papurello. Thévenin's battery model parameter estimation based on simulink. Energies, 15(17):6207, 2022.

[26] Thermal modeling of large format lithium-ion cells. Nerea Nieto, Luis Diaz, Jon Gastelurrutia, Isabel Alava, Francisco Blanco, Juan Ramos, and Alejandro Rivas.Journal of the Electrochemical Society, 160:A212–A217, 11 2012

[27] Research Progress of Battery Life Prediction Methods Based on Physical Model - Scientific Figure on ResearchGate.

[28] GitHub. 2024.DandeLiion data collected.